

See discussions, stats, and author profiles for this publication at: <https://www.researchgate.net/publication/221953768>

# Geochemical, isotopic, and remote sensing constraints on the origin and evolution of the Rub Al Khali aquifer system, Arabian Peninsula

Article in *Journal of Hydrology* · July 2008

DOI: 10.1016/j.jhydrol.2008.04.001

CITATIONS

31

READS

342

7 authors, including:



**Mohamed Sultan**

Western Michigan University

367 PUBLICATIONS 3,230 CITATIONS

[SEE PROFILE](#)



**Neil C Sturchio**

University of Delaware

394 PUBLICATIONS 10,156 CITATIONS

[SEE PROFILE](#)



**Saleh Alsefry**

Saudi Geological Survey

38 PUBLICATIONS 217 CITATIONS

[SEE PROFILE](#)



**Adam Milewski**

University of Georgia

131 PUBLICATIONS 795 CITATIONS

[SEE PROFILE](#)

Some of the authors of this publication are also working on these related projects:



Natural radioactivity in Sinai Groundwater [View project](#)



Sensitivity Analysis of the Groundwater Risk Index in the Middle East and North Africa Region [View project](#)



available at [www.sciencedirect.com](http://www.sciencedirect.com)



journal homepage: [www.elsevier.com/locate/jhydrol](http://www.elsevier.com/locate/jhydrol)



# Geochemical, isotopic, and remote sensing constraints on the origin and evolution of the Rub Al Khali aquifer system, Arabian Peninsula

M. Sultan <sup>a,\*</sup>, N. Sturchio <sup>b</sup>, S. Al Sefry <sup>c</sup>, A. Milewski <sup>a</sup>, R. Becker <sup>a</sup>,  
I. Nasr <sup>d</sup>, Z. Sagintayev <sup>a</sup>

<sup>a</sup> Department of Geosciences, Western Michigan University, Kalamazoo, MI, USA

<sup>b</sup> Department of Earth and Environmental Sciences, University of Illinois, Chicago, IL, USA

<sup>c</sup> Hydrology Division, Saudi Geological Survey, Jeddah, Saudi Arabia

<sup>d</sup> Desert Research Institute, Cairo, Egypt

Received 27 November 2007; accepted 1 April 2008

## KEYWORDS

Saudi Arabia;  
Rub Al Khali;  
Red sea hills;  
Groundwater recharge  
and discharge;  
Tropical rainfall mea-  
suring mission;  
Oxygen, hydrogen, and  
strontium isotopes

**Summary** Chemical and stable isotopic compositions of groundwater samples from the Rub Al Khali (RAK) in southern Saudi Arabia were analyzed. Samples were collected from wells of variable depth (1.5–800 m) along the perimeter of the eastern half of the RAK including flowing artesian wells, pumped wells (formerly artesian), and shallow hand-dug wells encompassing those in sabkha areas. Data indicate that the water from the artesian and formerly artesian wells represents the contents of confined aquifers. Such water (Group 1) is isotopically depleted ( $\delta^2\text{H}$  values ranging from  $-60\text{‰}$  to  $-35\text{‰}$ ), and has total dissolved solids (TDS) concentrations ranging from 1300 to 76,000 mg/L, indicating that much of the salinity is acquired in the subsurface. Water from shallow hand-dug wells including those in sabkha areas (Group 2) has experienced significant evaporation ( $\delta^2\text{H}$  values ranging from  $-34\text{‰}$  to  $+19\text{‰}$ ) as well as salinization (TDS as high as 92,000 mg/L) by dissolution of sabkha salts including halite and gypsum. Stable isotope data for the Group 2 water samples define an evaporation trend line originating from the Group 1 water samples. This relationship indicates that the Group 2-type water evolved from Group 1-type water by ascending through structural discontinuities, dissolving evaporative salts, and undergoing substantial near-surface evaporation in groundwater discharge zones (sabkhas) characterized by shallow groundwater levels ( $<2$  m). This interpretation is supported by the relatively unradiogenic Sr isotope ratios of groundwater samples ( $\text{Sr}^{87}/\text{Sr}^{86} = 0.70771\text{--}0.70874$ ) that are inconsistent with that of modern seawater ( $^{87}\text{Sr}/^{86}\text{Sr} = 0.70932$ ). The RAK aquifer water represents either high-elevation recharge

\* Corresponding author. Tel.: +1 269 387 5487.

E-mail address: [mohamed.sultan@wmich.edu](mailto:mohamed.sultan@wmich.edu) (M. Sultan).

from the Red Sea Hills, and/or recharge largely formed of paleo-water precipitated during moist climate intervals of the late Pleistocene recharging aquifers cropping out at the foothills of the Red Sea mountains. This inference is supported by a progressive decrease in hydraulic head and increase in groundwater salinity from west to east, substantial precipitation over the Red Sea Hills, and a major E–W trending channel network that channels precipitation from the Red Sea Hills toward recharge areas. Analysis of 3-hourly TRMM (Tropical Rainfall Measuring Mission: 1998–2006) precipitation data and digital elevation data shows that 27% of the average annual precipitation ( $150 \times 10^9 \text{ m}^3$ ) over the Arabian Peninsula is channeled toward the recharge zone of the RAK aquifer system, of which an estimated  $4 \times 10^9 \text{ m}^3 \text{ a}^{-1}$  to  $10 \times 10^9 \text{ m}^3 \text{ a}^{-1}$  of this water is partitioned as recharge to the RAK aquifer system. Additional integrated studies on recharge rates, sustainability, and water quality issues for the RAK aquifers could demonstrate that the RAK is one of the most promising sites for groundwater exploration in the Arabian Peninsula. Results highlight the importance of investigating the potential for sustainable exploitation of similar large aquifer systems that were largely recharged in previous wet climatic periods yet are still receiving modest modern meteoric contributions.

© 2008 Elsevier B.V. All rights reserved.

## Introduction

The low rates of precipitation (<100 mm/yr) over many of the arid and hyper-arid parts of the world represent a serious challenge to organized efforts to populate and develop such areas. This problem is exemplified in the Saharan belt and in the Arabian Peninsula. At present, precipitation over the Sahara and the Arabian Peninsula is largely localized in high-elevation areas (e.g., Red Sea Hills in Egypt, Sudan, and Arabia), whereas the majority of the remaining lands in this area receive very little, if any precipitation. The current conditions contrast with the wet climatic periods that prevailed throughout the Late Pleistocene. In this manuscript, we show that large aquifers that were mainly recharged during wet periods and are still receiving modern contributions from localized precipitation can potentially provide opportunities for sustainable development.

Underlying the vast deserts of the Rub Al Khali (RAK), meaning the 'Empty Quarter', is one of the largest aquifer systems of the arid world, the Rub Al Khali Aquifer System (RAKAS) of the Arabian Peninsula. This aquifer extends for some 650,000 km<sup>2</sup> in the southern third of the Arabian Peninsula in southern Saudi Arabia, Oman, Yemen, and United Arab Emirates (Fig. 1). With the exception of a few settlements at the outskirts of the desert, the RAK remains largely uninhabited and undeveloped because of its harsh climatic conditions (temperatures > 50 °C in summer) and largely inaccessible terrain. The RAK encompasses the largest dune fields on Earth with some dunes reaching hundreds of meters high. These problems together with a lack of understanding of the area's groundwater potential have hindered plans for its development. In this manuscript, we present the results of a preliminary integrated investigation, involving geochemical, isotopic, field, and remote sensing data that addresses the origin and evolution of the groundwater of the RAKAS.

Understanding the origin, evolution, and magnitude of this major groundwater resource is crucial for optimal management of the RAK. This paper summarizes geochemical and isotopic data for 24 groundwater samples obtained during a sampling expedition to the RAK in February/March

2006. Interpretation of geochemical and isotopic data was conducted in the context of relevant geologic and hydrogeologic data sets including: spatial variations in hydraulic head, distribution of recharge areas (extracted from geologic maps), distribution of watersheds and drainage networks (extracted from digital elevation data), and temporal precipitation over the watersheds. The latter was extracted from 3-hourly TRMM (Tropical Rainfall Measuring Mission) precipitation data for a nine year time period of 1998–2006. We also show that there are indications that groundwater resources in the RAK are apparently significant compared to other areas in the Peninsula and offer development potential that merits further detailed investigations.

## Geology, hydrogeology, landforms, and climate of the RAK

To date, only limited detailed studies have been conducted on the hydrogeology of the RAK in Saudi Arabia. These inadequacies will be addressed in part by examining our data sets in the context of the more thoroughly studied portions of the RAK in neighboring countries (United Arab Emirates and Oman) and that of areas of similar hydrogeologic and climatic settings in neighboring countries. Such an approach could potentially provide insights into the origin and evolution of groundwater in the study area.

Precambrian crystalline basement of the Arabian Shield crops out along the eastern margins of the Red Sea coastline forming the westernmost margin of the RAK terrain. The basement complex rocks are impermeable and groundwater in basement areas is found in fractures or in the alluvial aquifers within the wadi network dissecting these domains. Unconformably overlying the crystalline basement are thick sequences of sedimentary formations ranging in age from Cambrian to recent; they dip gently to the east and thicken in the same direction reaching thicknesses of up to 5 km in the vicinity of the Persian Gulf. These stratigraphic relationships are demonstrated in Fig. 2, a generalized schematic cross-section along a SW to NE trending transect.

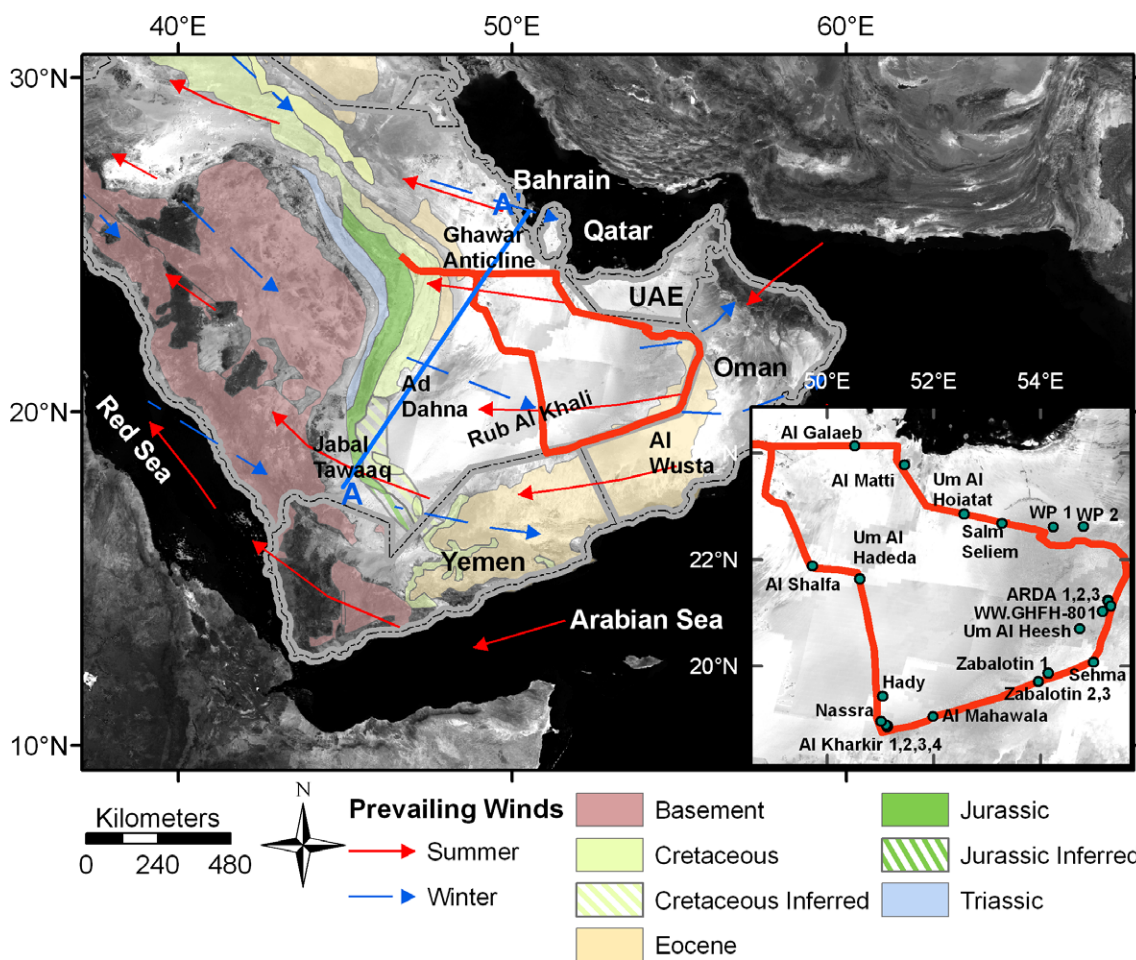


**Figure 1** Satellite image showing the areal extent of the RAK in Saudi Arabia, Yemen, and United Arab Emirates. The figure also shows the general distribution of major rock units in the area (modified from AlSharhan and Nairn, 1997; Powers et al., 1966) and the prevailing wind patterns (Dewdney, 1988). Inset: sample locations (blue dots) together with the traverse (red line) along which samples were collected. A schematic cross section along line A–A' is shown in Fig. 2.

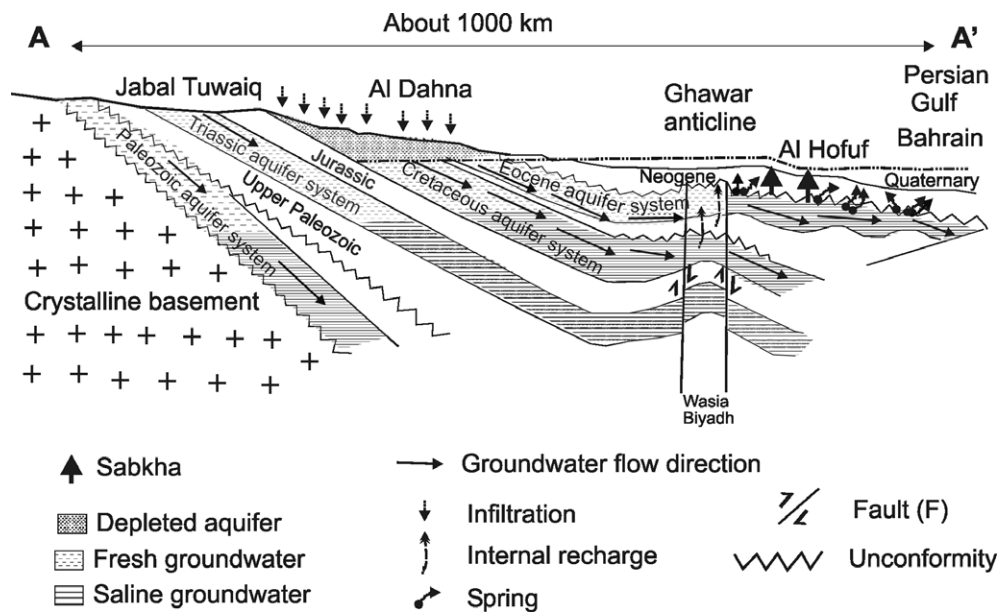


**Figure 2** A SW to NE schematic cross section through the RAK along line A–A' in Fig. 1 modified from Beaumont (1977) and AlSharhan et al. (2001).

Groundwater in the RAK is hosted primarily in sandstone, limestone, and dolomite formations separated by interleaving confining shale units. These aquifers are here grouped in: (1) Paleozoic sandstone aquifers (e.g., Wajid aquifer: 200–900 m thick) and limestone and dolomite aquifers of the Kuff formation (250–600 m), (2) Mesozoic sandstone aquifer (e.g., Minjur: 400 m thick; Biyadh-Wasia: 425 m), and (3) Cenozoic (Eocene and Neogene) limestone and dolomite (e.g., Umm er Radhuma: 250–700 m; Dammam: 250 m) (Al Alawi and Abdulrazzak, 1994; AlSharhan et al., 2001; Ministry for Higher Education, 2000).

These sedimentary formations are exposed in the foothills of the Red Sea Hills providing ample opportunities for groundwater recharge for all aquifers (Cambrian to Quaternary) from rain precipitating over the Red Sea Hills and surroundings. Precipitation is concentrated over the mountain ranges and/or highlands surrounding the area from the west (Red Sea Hills), east (Oman mountains), south (e.g., Hadramount and Dhofar mountains), and north (Yabrin mountains) and is channeled by an extensive E–W trending watershed intercepting the recharge areas. These relationships are demonstrated in Fig. 3a, which shows a mosaic of Landsat Thematic Mapper scenes draped over digital elevation data for the RAK and surrounding mountains and a similar drape for the major watersheds and drainage networks in the area (Fig. 3b). The precipitation over the southern and eastern highlands is less likely to recharge the aquifer sequence in its entirety since only the more recent aquifers

(Cenozoic) crop out at the foothills of these mountain ranges.

Radiocarbon dating of groundwater samples from a number of these reservoirs (Saq: 22,000–28,000 ka; Biyadh-Wasia: 8000–16,000 ka; Umm er Radhuma: 10,000–28,000 ka) have lead to interpretations suggesting that these reservoirs were recharged during previous wet climatic periods in the Quaternary (AlSharhan, 2003; Beaumont, 1977; Otkun, 1971). Although we believe that the aquifers are largely formed of fossil water, we suggest that during the intervening dry periods, as is the case now, these aquifers must receive additional recharge given the relatively high precipitation over the Red Sea Hills and the presence of a network of ephemeral streams that can channel these waters to the recharge areas at the foothills of these mountains. This has been demonstrated to be the case in similar settings in the Eastern Desert of Egypt and the Sinai Peninsula (Sultan et al., 2007).

### Sample locations and methodology

A set of water samples from 24 locations was collected along a traverse that covered the eastern half of the RAK from locations shown in the inset of Fig. 1. The sample locations are between latitudes 19° and 24°N, and longitudes 50° and 56°E. Samples are grouped in two groups, Group 1 and Group 2. Group 1 samples are from deep (>150 m deep) groundwater aquifers and were collected from flowing artesian (e.g., ARDA 1, ARDA 3, WW.GHFH-801, Zabalotin 2, Al Mahawla, Al Kharkhir 4), pumped wells (e.g., ARDA 2, Sehma Army well, Zabalotin 1, Al Shalfa), and springs (e.g., Um El Heesh, Al Matti). Many of these wells discharge hot waters (temperatures of up to 50 °C) and display an H<sub>2</sub>S odor. Group 2 samples are from shallow production wells (e.g., Um Al Hoitat, Salem Seleim), hand-dug wells (Al Galeab, Al Kharkhir1,2,3, Nassra, and Hady), and water points (WP 1 and 2).

Three samples were collected at each location: (1) a filtered, acidified 60-mL sample for cation analyses; (2) an unfiltered, unacidified 125-mL sample for anion and alkalinity analyses; and (3) an unfiltered, unacidified 30-mL sample for stable isotope ratio analyses for hydrogen and oxygen.

Cations were analyzed by inductively coupled plasma-atomic emission spectrometry. Anions were analyzed by ion chromatography. Alkalinity was determined by titration. Hydrogen and oxygen isotope ratios were determined by the methods of Coleman et al. (1982) and Socki et al. (1992), respectively. Hydrogen and oxygen isotope ratios are expressed in the conventional  $\delta$  (delta) notation, where

$$\delta = [(R_{\text{sample}}/R_{\text{standard}}) - 1] \times 1000 \quad (1)$$

and  $R$  represents the ratio of deuterium/hydrogen (D/H) or <sup>18</sup>O/<sup>16</sup>O, respectively, in the sample and the standard. The resulting sample values of  $\delta$ D and  $\delta$ <sup>18</sup>O are reported in units of ‰ (per mil), or parts per thousand deviation relative to the corresponding ratios in Standard Mean Ocean Water (V-SMOW) (Coplen, 1996).

Strontium isotope ratios were measured by dynamic multicollecion on a VG Sector 54 thermal ionization mass spectrometer. Strontium was concentrated from water samples and purified using extraction chromatography, and then

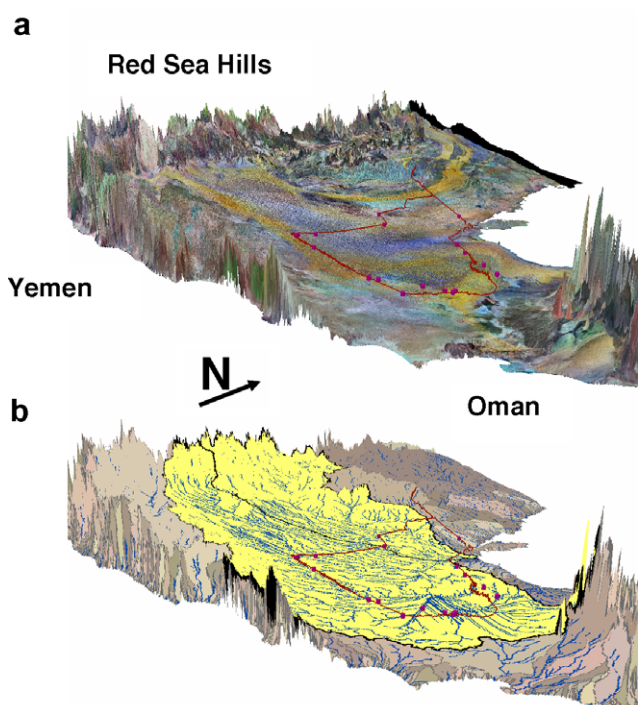


**Figure 3** 3-D representations. (a) Landsat TM false color images draped over vertically exaggerated digital elevation data (1 km SRTM). Also shown in Fig. 3a are our sample locations (red dots) and field trip traverse (red line). (b) Watersheds (RAK watershed: yellow area) and drainage networks extracted from SRTM data draped over 1 km SRTM data.

loaded onto Re filaments with  $\text{H}_3\text{PO}_4$  and  $\text{TaCl}_5$  activator. Procedural Sr blanks were  $<40$  pg. The  $^{87}\text{Sr}/^{86}\text{Sr}$  of NIST 987 obtained during the period of these analyses is  $0.710246 \pm 0.000011$  ( $2\sigma$ ), with  $^{88}\text{Sr}$  current maintained at  $3 \times 10^{-11}$  amps.

### Stable and radiogenic isotope geochemistry in RAK groundwaters

Hydrogen and oxygen isotope ratios are ideal tracers of the origin and evolution of groundwater because they compose the water molecules and are sensitive to physical processes such as atmospheric circulation, groundwater mixing and evaporation (Clark and Fritz, 1997; Dansgaard, 1964). The isotopic composition of precipitation varies as a function of elevation and therefore the source of groundwater recharge in an area with significant topographic variation can be identified from its isotopic composition. The stable isotope ratios of hydrogen and oxygen for the RAK groundwater samples are shown in Table 2 and Fig. 4. Also shown in Fig. 4 are data for mean annual precipitation from an IAEA monitoring station in Bahrain as well as data from a study of rainfall isotopic composition in Oman (Macumber et al., 1994). The RAK groundwater samples have a wide range in hydrogen and oxygen isotope ratios, from a relatively depleted composition of  $\delta\text{D} = -60.2\text{‰}$ ,  $\delta^{18}\text{O} = -6.6\text{‰}$  for Al Matti artesian well to a relatively enriched composition of  $\delta\text{D} = +19.2\text{‰}$ ,  $\delta^{18}\text{O} = +11.6\text{‰}$  for a shallow hand-dug water pit within a sabhka area (Tables 1 and 2; water point 2).

A general isotopic distinction is apparent between samples from groups 1 and 2: Group 1 samples are isotopically depleted, having  $\delta^2\text{H}$  values ranging from  $-60\text{‰}$  to  $-35\text{‰}$ , whereas Group 2 samples are more enriched having  $\delta^2\text{H}$  values ranging from  $-34\text{‰}$  to  $+19\text{‰}$ . Group 1 compositions could represent either high-elevation recharge from moun-

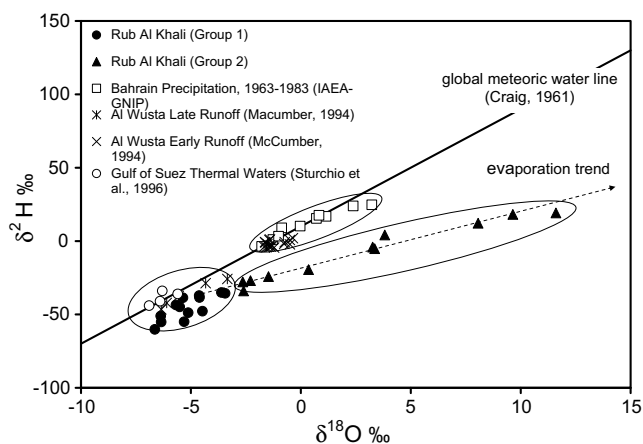


**Figure 4** Stable isotope ratios of hydrogen ( $\delta\text{D}$ ) vs. oxygen ( $\delta^{18}\text{O}$ ). Group 1 and Group 2 samples from the RAK (this study) are compared to Sinai's geothermal groundwater (Sturchio et al., 1996), early and late runoff from a monsoonal tropical cyclone that crossed Al-Wusta region in central Oman in late September to early October 1992 (Macumber et al., 1994), and precipitation from the IAEA station in Bahrain (IAEA and WMO, 2004). Also shown is the Global Meteoric Water Line (Craig, 1961).

tainous areas to the west of the RAK, and/or recharge largely formed of paleo-water precipitated during moist climate intervals of the late Pleistocene.

The isotopic composition of moisture in northwesterlies and monsoonal precipitation have been evaluated for areas lying at the peripheries of the RAK (e.g., Matter et al., 2006; Weyhenmeyer et al., 2002), however isotopic analyses for such precipitation over the Red Sea Hills and the RAK at large has not been characterized. In the absence of such data, it is difficult to ascertain whether the water in the Group 1 samples was generated due to the intensification of monsoons and northward migration of the monsoonal rainfall belt during previous wet climatic periods (Burns et al., 2003; Fleitmann et al., 2003a,b; Fleitmann et al., 2004; Preusser et al., 2002) or due to the intensification of paleo-northwesterlies at the expense of a retreating monsoonal front (Leuschner and Sirocko, 2000). Because modern precipitation over the lowlands of the RAK is sparse, intensified precipitation during previous wet climatic periods most likely has played an important role in recharging the RAKAS, a notion supported by ages of groundwater in the study areas and by the presence of late Pleistocene and Holocene lake deposits in the area (McClure, 1978, 1980).

Regardless of whether it was the monsoons or the northwesterlies that generated the rain that produced Group 1 groundwater compositions, precipitation most likely originated at high altitudes over the surrounding mountains and/or as precipitation from clouds that traveled for long distances inland to reach recharge areas within the RAK. In either case, the isotopic composition of this precipitation should be depleted compared to precipitation along adjoining lowlands and coastal regions. The expected depletion of isotopic compositions associated with continental and altitude effects can probably explain why the isotopic composition for the RAK Group 1 groundwater is depleted compared to low-elevation precipitation at Bahrain, an island within the Arabian Gulf (Fig. 4). If the clouds that produced the precipitation at Bahrain were to cross the RAK, precipitation from such clouds over the Red Sea Hills could conceivably produce rain with isotopic compositions similar to those of Group 1 given that the Red Sea Hills reach over 2 km in height (altitude effect:  $-2.8\text{‰}/\text{km}$ ) (Poage and Chamberlain, 2001) and monsoonal fronts can travel distances exceeding 1000 km (continental effect:  $-0.2$  to  $-0.4\text{‰}/100$  km) (Dansgaard, 1964) before reaching the Red Sea Hills (Fig. 1). Our Group 1 samples are similar with respect to their isotopic compositions to the Gulf of Suez thermal waters (Fig. 4). The isotopic depletion of these thermal waters is likely to have resulted in part from high altitude precipitation over the Red Sea Hills in southern Sinai and/or from transcontinental effects as the intensified paleo-westerlies crossed the Sinai Peninsula in Pleistocene wet climatic periods (Issar and Bruins, 1983).

The depletion of the Group 1 isotopic compositions may not be solely related to the altitude and/or transcontinental effects; the amount effect (Dansgaard, 1964) might play a role as well. Macumber et al. (1994) reported isotopic compositions for a heavy rainfall event from a tropical cyclone (monsoonal origin) that crossed Al-Wusta region (Fig. 1) in central Oman in late September and early October of 1992. The early runoff had enriched isotopic compositions similar to those

**Table 1** Sample locations and field data

#	Name	Long	Lat	Type	Depth WT (m)	TDepth (m)	Temp (°C)	Smell	TDS (ppm)	Cond. ( $\mu\text{S}/\text{cm}$ )
1	Al Galaeb	50.5194	24.1388	Hand dug	11.8	13			3160	4860
2	Al Matti	51.4438	23.7761	Spring	Flowing			H <sub>2</sub> S	10,800	16,620
3	Um Al Hoiatat	52.5633	22.8648	Well	3.93				23,700	36,500
4	Salm Seliem	53.2738	22.6831	Well	5	16			16,400	25,300
5	Water Point1	54.2450	22.6142	Water point	0.4	1.5			91,900	141,400
6	Water Point2	54.8055	22.6244	Water point	1.75	3			Over range	
7	ARDA 1 Well (7-S-27)	55.2649	21.2373	Well	Flowing	>400	42	H <sub>2</sub> S	11,380	17,430
8	ARDA 2	55.2716	21.2219	Well	10	>200?	32		22,400	34,400
9	ARDA 3	55.3286	21.1351	Well	Flowing	>300	>35	H <sub>2</sub> S	76,100	11,7100
10	WW.GHFH-801	55.1605	21.0288	Well	Flowing	>400	44	H <sub>2</sub> S	10,700	16,460
11	Um Al Heesh Spring	54.7325	20.7051	Spring	Flowing			H <sub>2</sub> S	6240	9600
12	Sehma Army Well	54.9927	20.0732	Well	28	>200	34		6890	10610
13	Zabalotiin 1 Well	53.9646	19.7042	Well	14	>400	47	H <sub>2</sub> S	2990	4620
14	Zabalotin 2 (ARAMCO Well)	53.9640	19.7107	Well	Flowing	>400	44	H <sub>2</sub> S	2370	3650
15	Zabalotin 3 (Al Khasfa)	54.1502	19.8714	Hand dug	2.4	10			7340	11,280
16	Al Mahawala WW.KRKR-803	51.9854	19.0571	Well	Flowing	>400	50	H <sub>2</sub> S	1330	2050
17	Al Kharkir 1	51.1232	18.8565	Hand dug	3.7	5.85			9700	14910
18	Al Kharkir 2	51.1414	18.8766	Hand dug	3.5	16			3810	5890
19	Al Kharkir 3	51.1274	18.8557	Hand dug	30	800	48	H <sub>2</sub> S	1490	2310
20	Al Kharkir 4 Well	51.1026	18.8978	Well	>150 m	450	45	H <sub>2</sub> S	1540	2380
21	Nassra Well	51.0051	18.9641	Hand dug	3.2	4.95			6500	9970
22	Hady	51.0390	19.4377	Hand dug	15.7	32			7470	11,480
23	Um Al Hadedda Well	50.6031	21.6424	Hand dug	14.25	25			4450	6880
24	Al Shalfa	49.7138	21.8783	Well	40	150			568	841

reported from Bahrain, but the runoff following the rains of the 4th and 5th of October were depleted and compositionally similar to those we measured for Group 1 samples (Fig. 4).

It is likely that many of the Group 2 samples were originally of Group 1 origin (i.e., surface groundwater discharge), but affected by substantial amounts of evaporation as well as dissolution of evaporative salts that are widespread in the subsurface and at the surface sabkha areas. This interpretation is supported by the occurrence of the Group 2 samples along an evaporation trend line (Fig. 4) that extends upward from the Group 1 samples. Where a number of samples were collected from both deep wells and near-surface wells at the same location, isotopic enrichments indicative of evaporation were observed in the near-surface samples. For example, the isotopic composition of Zabalotin 3, a shallow (total depth: 10 m, depth to water table: <2.5 m) hand-dug well is best interpreted as resulting from evaporation of groundwater of isotopic compositions similar to Zabalotin 1 (total depth: 400 m; depth to water table: 14 m) and Zabalotin 2 (total depth: >400 m; flowing). Similarly, the isotopic composition of the shallow (depth to water table: <4 m) hand-dug Al Kharkir 1 (total depth: 6 m; depth to water table: <4 m) and Al Karkir 2 (total depth: 16 m; depth to water table: <4 m) are best interpreted as resulting from evaporation of groundwater of isotopic composition similar to that of the deep Al Kharkir 3 (total depth: 800 m; depth to water table: 30 m) and Al Kharkir 4 (total depth: 450 m; depth to water table: >150 m) well samples.

The effect of evaporation on the isotopic composition of water from both open water bodies and from unsaturated sand or soil columns has been studied by Allison (1982). Alli-

son (1982) concluded that slopes ranging from about 3 to 5 on a  $\delta^2\text{H}$  vs.  $\delta^{18}\text{O}$  diagram (such as Fig. 4) are indicative of progressive evaporation, where the lower values (slope near 3 or 4) are more characteristic of evaporation in an unsaturated sand or soil whereas the higher values (slope near 5 or 6) are characteristic of evaporation of open water bodies such as lakes or streams. The slope of the evaporation trend shown in Fig. 4 is about 4, suggesting that most of the evaporation in the RAK is occurring through unsaturated sand or soil, which is consistent with the occurrence of many of Group 2 samples in the shallow subsurface and in moist sabkha areas with abundant presence of evaporative salt deposits and calcretes. These relationships are demonstrated in Fig. 5 and Tables 1 and 2 which show that the most evaporated ( $\delta^2\text{H} > 18$ ) of Group 2 samples (water points 1 and 2) were collected from areas previously mapped as sabkhas (USGS and Aramco, 1963) and are characterized by the shallowest groundwater levels (<2 m).

The depth (from surface) to water table contours shown in Fig. 5 were extracted from groundwater data from 156 oil prospecting wells drilled by Aramco tapping the Paleozoic (2 wells), Triassic (1 well), Cretaceous (11 wells), and Tertiary (142 wells) aquifers (Dimock, 1961). It is suggested here that these relationships could indicate that many of the active sabkhas (e.g., area encompassing water points 1 and 2) represent domains of groundwater discharge for the RAK groundwater aquifers. We speculate that mapped sabkhas south of water points 1 and 2 could have formed at relatively higher elevations during previous wet climatic periods when groundwater levels were higher than nowadays.

The notion that the distribution of sabkha could largely represent active and previous areas of groundwater dis-

**Table 2** Chemical and isotopic analyses of RAK groundwater

Name	Ca (mg/L)	Mg (mg/L)	Na (mg/L)	K (mg/L)	Cl (mg/L)	HCO <sub>3</sub> (mg/L)	SO <sub>4</sub> (mg/L)	TDS (mg/L)	δ <sup>18</sup> O (‰)	δ <sup>2</sup> H (‰)	Sr (ppm)	1/Sr	<sup>87</sup> Sr/ <sup>86</sup> Sr <sup>a</sup> (‰)	Group
1 Al Galaeb	504.6	76.1	576.8	57.7	491.6	35.4	2200	3160	3.82	4.2				2
2 Al Matti	847	372.6	2380	90.6	4261.6	31.8	2730.1	10,800	-6.64	-60.2	16.99	0.059	0.70785	1
3 Um Al Hoiatat	4099.5	2344	100380	2512.5	178000	13.7	1440	<200,000	8.06	12.2	18.54	0.054	0.70874	2
4 Salm Seliem	941.6	420.8	7115	160.3	12041.5	72.78	4083.4	23,700	3.36	-5.1	14.37	0.07	0.70858	2
5 Water Point1	645.5	351.2	4875	130.2	7418.5	52.7	3213.9	16,400	11.6	19.2	59.92	0.017	0.70865	2
6 Water Point2	1720	1170.5	39366	1030.4	65107.9	33.04	2840	91,900	9.64	18.2	110.5	0.009	0.70869	2
7 ARDA 1	452.3	260	2875	85.1	5477.2	181.55	766.5	11,380	-6.35	-55.1	33.74	0.03	0.70771	1
8 ARDA 2	565.4	262.8	6847.5	140.2	11839.8	97.66	1495.3	22,400	-3.44	-43.5	26.36	0.038	0.7079	1
9 ARDA 3	1124	583.8	31836	981.6	49566.1	249.5	8700	76,100	-5.68	-51.1				1
10 WW.GHFH-801	472.2	286.3	2667.5	79.9	5107.9	197.4	800.9	10,700	-6.37	-55				1
11 Um Al Heesh Spring	816.6	150.8	1282.5	53.8	2109.9	66.8	2243.7	6240	-5.31	-47.8				1
12 Sehma Army Well	742.6	208	1492.5	52.5	2376.3	132.5	2398.6	6890	-4.47	-38.6				1
13 Zabalotin 1	239.1	111.6	567.6	33.9	861.5	112.5	887	2990	-5.36	-44.9				1
14 Zabalotin 2	195.1	126	424.6	33.9	653.4	111.48	760	2370	-5.51	-48.8				1
15 Zabalotin 3	678.3	272.5	1670	86.9	2320.6	77.34	2726.5	7340	-3.61	-37.1				1
16 Al Mahawala	149.2	89.4	156.8	10.5	215.2	209.6	485.6	1330	-5.12	-38.5				1
17 Al Kharkir 1	596	635.5	2360	84.3	2874.6	213.11	4655	9700	-1.47	-24.2				2
18 Al Kharkir 2	594.1	193.6	622.8	29	738.6	83.6	2181.8	3810	-2.64	-27.8				2
19 Al Kharkir 3	237	111.8	131.8	14.3	204.2	153.1	769.9	1490	-4.62	-35.6				1
20 Al Kharkir 4 Well	246.4	124.6	132.7	16.2	204.5	152.9	850.4	1540	-4.61	-35.1				1
21 Nassra Well	629.4	266.5	1490	47.3	1448.1	78.8	3133.2	6500	0.35	-19.4				2
22 Hady	634	256.7	1835	56.6	2197.3	68.15	3166.7	7470	3.27	-4.1				2
23 Um Al Hadedra Well	234	100.7	1135	25.9	1579.6	67.78	801.5	4460	-2.29	-34				2
24 Al Shalfa	18.1	5.5	148.3	3.5	126.6	180.1	66.2	568	-2.6	-26.9				2

<sup>a</sup> Precision of Sr isotope ratios is ±0.00001.

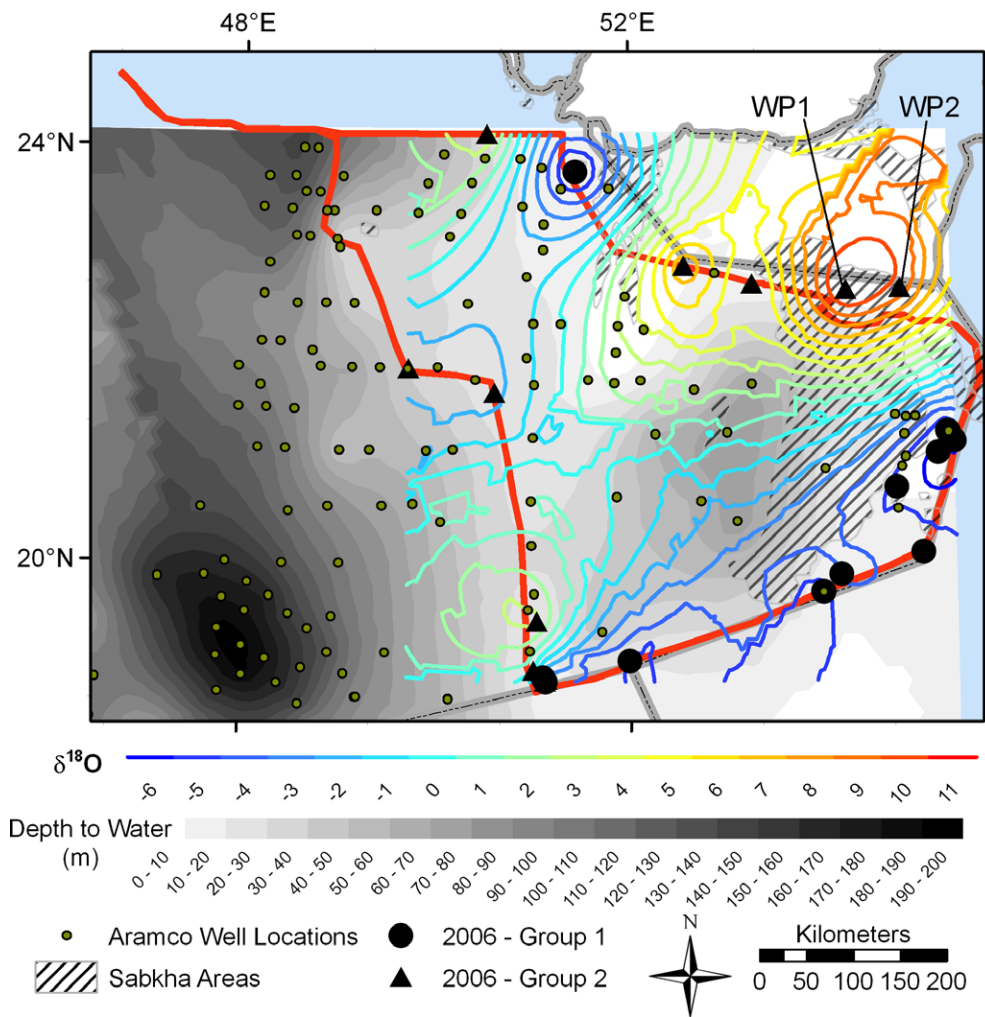


**Figure 5** Spatial variations in  $\delta^{18}\text{O}$  values for our groundwater samples and depth to water table extracted from the Aramco well data set. The depth (from surface) to water table contours were extracted from groundwater data from 156 oil prospecting wells drilled by Aramco tapping the Paleozoic (2 wells), Triassic (1 well), Cretaceous (11 wells), and Tertiary (142 wells) aquifers (Dimock, 1961). Additional data (TDS and static head) from the same wells are given in Fig. 8. Also shown is the distribution of sabkhas (USGS and Aramco, 1963).

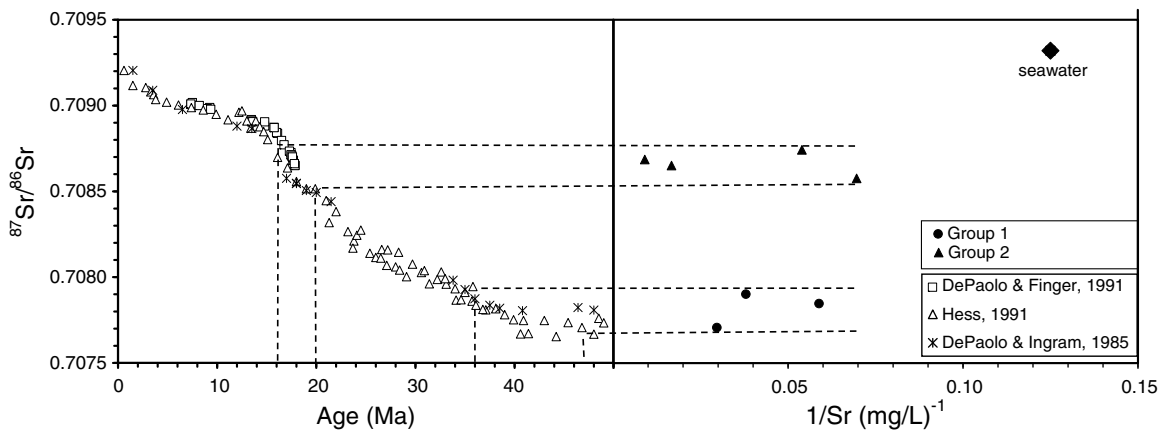


**Figure 6**  $^{87}\text{Sr}/^{86}\text{Sr}$  ratios versus  $1/\text{Sr}$  concentrations (mg/L) for Group 1 and Group 2 groundwater samples that are proximal (<200 km) to the Gulf. Group 1 samples have Sr isotope ratios similar to Eocene seawater, and Group 2 samples have Sr isotope ratios similar to Neogene seawater, indicating significant water–rock interaction within Eocene and Neogene aquifers, respectively. Variations in Sr isotopic ratios through time for seawater were extracted from Depaolo and Finger (1991), Hess et al. (1991) and Depaolo and Ingram (1985).

charge as opposed to representing coastal sabkha settings affected by mixing with seawater as previously suggested (Glennie, 1970) is further tested by examining the Sr isotope systematics in a representative suite of our groundwater samples. Seven groundwater samples classified as Group 1 (Al Matti, ARDA 1, 2) and Group 2 samples (Um Al Hoitat, Salem Seliem, water points 1 and 2) that were collected from locations proximal (<200 km) to the Gulf were analyzed for their  $^{87}\text{Sr}/^{86}\text{Sr}$  compositions and Sr concentrations (Table 2; Fig. 6).  $^{87}\text{Sr}/^{86}\text{Sr}$  ratios are less radiogenic (0.70771 to 0.70874) and Sr concentrations are high (14.4 to 59.9 ppm) compared to modern seawater compositions ( $^{87}\text{Sr}/^{86}\text{Sr} = 0.70932$  and  $\text{Sr} = 8$  ppm) and no obvious mixing trends with modern seawater composition are observed suggesting that these sabkhas are not marine in origin. Central to understanding the hydrologic setting (recharge, transport, and discharge) of the RAK groundwater is the origin and evolution of the solutes of these waters.

### Chemical composition of groundwaters

Chemical data for the 24 water samples collected in this study are listed in Table 2. The samples have a wide range concentration of total dissolved solids (~600–92,000 mg/L) that is dominated by a Na–Ca–Cl– $\text{SO}_4$  salt assemblage.

It is useful to compare certain ionic ratios in groundwater samples with unfractionated marine aerosols (essentially seawater ion ratios) to assess sources of solutes. For example, the observed correlations between Na and Cl (Fig. 7a) indicate that marine aerosols or marine evaporites (i.e. halite) are most likely a dominant source of solutes. Marine aerosols may be deposited as dry salts on the land surface, and periodically dissolved and transported downward toward the aquifer during sporadic rainfall events. Some of these solutes may be concentrated by evaporation as halite, gypsum, and other salts within the soil layers and unsaturated alluvial deposits; these evaporite salts may accumulate for many years, eventually being dissolved transported to the groundwater aquifer when a sufficiently strong rainfall event occurs. While this scenario could be readily used to explain the concentrations of Na and Cl in a number of our Group 1 groundwater samples with low to moderate concentrations (e.g., samples 11–15, Table 2), it is more difficult to invoke such a process for other samples (e.g., samples 8 and 9, Table 2) showing much higher concentrations of these elements. Some other processes are needed to account for the observed high Na and Cl concentrations in such samples, such as evaporite dissolution in the subsurface and near-surface evaporation.

Comparison of  $\delta^2\text{H}$  values vs. chloride concentrations (Fig. 7b) shows several key features of RAK groundwaters. Fig. 7b compares Group 1 and Group 2 samples with different symbols to illustrate the possible relationships between the two groups. Also shown in Fig. 7b is seawater composition, halite saturation, and an evaporation trend. The evaporation trend shown is for evaporation of dilute water having  $\delta^2\text{H} = -60\text{‰}$  and  $\text{Cl} = 7.5$  mg/L, which is representative of precipitation on the Arabian Peninsula at high elevation. Evaporation of water having higher initial Cl concentration would produce an evaporation trend line parallel to the one shown in the figure, but displaced to the right. First, this diagram shows that Group 1 waters have a high range in

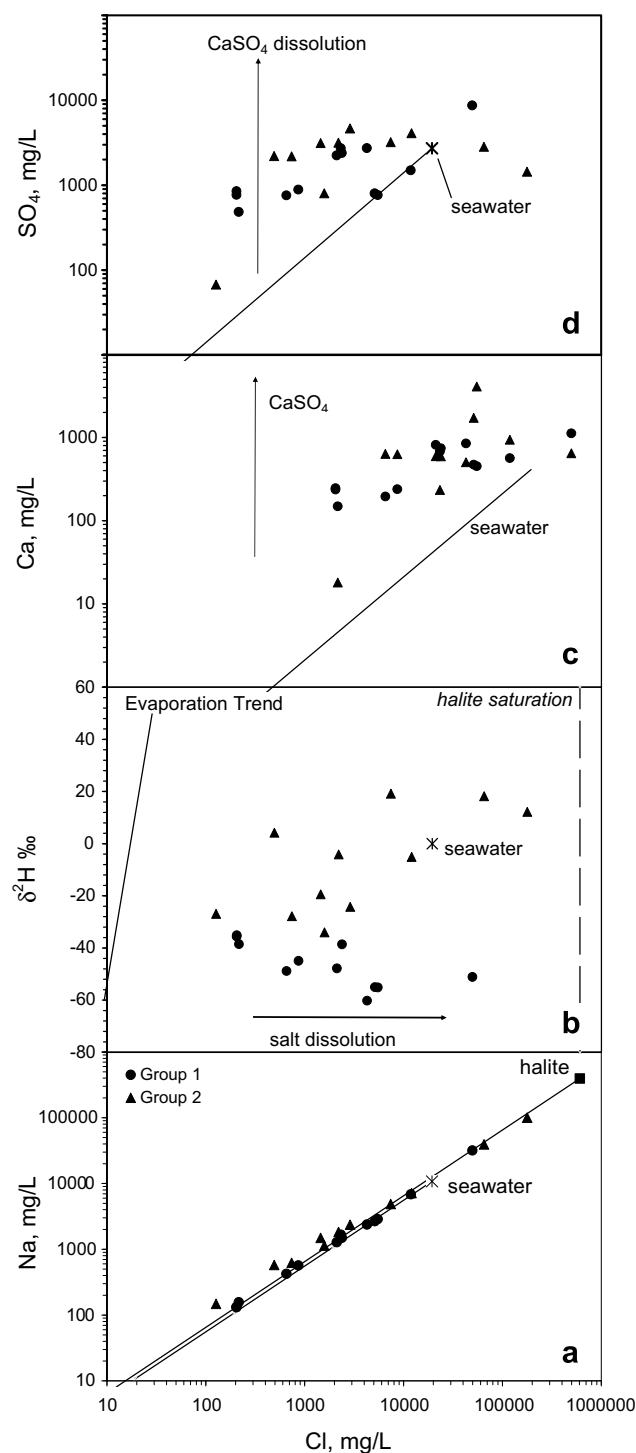


**Figure 7** Solute concentrations in mg/L in the RAK groundwater. (a) Na versus Cl, (b)  $\delta\text{D}$  versus Cl, (c) Ca versus Cl, and (d)  $\text{SO}_4$  versus Cl. Seawater dilution line represents unfractionated marine aerosols.

salinity, and the most saline Group 1 waters have the lowest  $\delta^2\text{H}$  values. This indicates that the Group 1 waters probably acquire much of their salinity in the subsurface. Second, all Group 2 samples have  $\delta^2\text{H}$  values that are equal to or greater than Group 1 samples having the same Cl concentrations. This indicates that all Group 2 samples could be produced by evaporation of Group 1 samples. Mixing with

seawater is contradicted by the observed relationship between  $\delta^2\text{H}$  and salinity, especially for Group 1 waters, indicating that seawater intrusion does not play a major role in salinization of groundwater at the sampled locations.

The sources of salinity in the RAK groundwaters can be constrained further by considering the deviation of solute compositions from those derived strictly from marine aerosols. For example, Fig. 7d shows the relation between sulfate and chloride concentrations, and there is a strong enrichment of sulfate relative to that which can be attributed to marine aerosols. The most likely source for this sulfate is from dissolution of anhydrite or gypsum in the subsurface (for Group 1 samples) or in the shallow near-surface environment (Group 2 samples). Additional evidence supporting Ca mineral dissolution as a major contribution to salinity is given by the relationship between Ca and Cl concentrations as shown in Fig. 7c. Fig. 7c and d indicates that there are about the same Ca and  $\text{SO}_4$  concentrations in samples having 1000 mg/L Cl as in samples having 10,000 mg/L Cl, so the Ca and  $\text{SO}_4$  concentrations are likely being controlled by mineral dissolution instead of fluid mixing.

Group 1 samples could have acquired much of their solutes in the subsurface from interaction with aquifer rock units along their flow paths by ion exchange reactions (e.g., Appelo, 1994; Chapelle and Knobel, 1983) and by dissolution of evaporites. A likely candidate is the Hormoz Series, an Upper Proterozoic sedimentary sequence (2 km thick) that underlies all major oil fields in the Persian Gulf area and surroundings. It is largely formed of bedded salt, gypsum, anhydrite, with thick interbeds of dolomite, shale, and sandstone. This scenario is supported by: (1) a

general west to east increase in total salinity from the Aramco well data set (Dimock, 1961) (Fig. 8a) and in our groundwater samples (Fig. 8b), and (2) the correspondence between the distribution of the highest salinities in groundwater data with the distribution of the Hormoz series at depth (Fig. 8a and b). In addition, there are evaporite beds within the lower Eocene Rus Formation which underlies the productive aquifer of the Middle Eocene Dammam Formation. Strontium isotope ratios of the Group 1 samples (Table 2) match those of Eocene seawater at 35–45 Ma (Fig. 6), indicating that the Group 1 water samples analyzed for Sr isotope ratios may have had significant residence time and water–rock interaction within the Dammam aquifer.

Group 2 samples (but not Group 1 samples) are subject to additional salinization by concentration of solutes by evaporation in near-surface sabkha environments and dissolution of evaporites that form in such areas. The Group 2 samples analyzed for Sr isotopes (Table 2) have  $^{87}\text{Sr}/^{86}\text{Sr}$  ratios consistent with lower Neogene seawater at 15–20 Ma (Fig. 6), indicating that they may have had significant residence time and water–rock interaction within the Neogene aquifer that overlies the Dammam aquifer. The most saline of Group 2 samples, samples WP1 and WP2, were sampled from areas mapped as sabkhas (Fig. 8a and b).

Additional insights into the sources of groundwater and mechanics of recharge were obtained by extraction and analysis of data pertaining to modern precipitation and distribution of watersheds and drainage networks over the RAK and surroundings. Such an understanding of the extent of modern recharge in the RAK is also critical to the evalua-

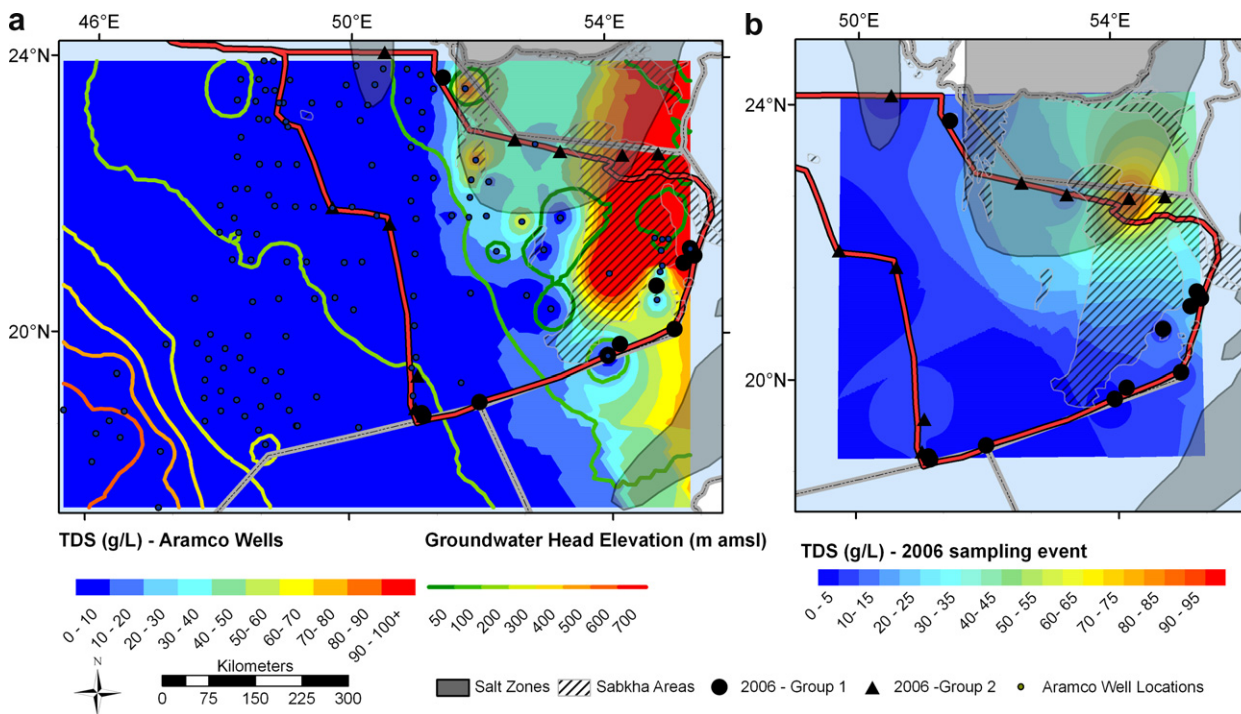


**Figure 8** Spatial variations in total dissolved solids, and static head data across the RAK: (a) total dissolved solids in groundwater and static head data distribution from 156 oil exploration wells drilled by Aramco in the RAK (Dimock, 1961) and (b) total dissolved solids in Groups 1 and 2 groundwater samples. Also shown is the distribution of sabkhas (USGS and Aramco, 1963) and the Hormoz salt formation in the subsurface (modified from Edgell, 1991).

tion of the groundwater development potential for the RAK groundwater.

### Modern contributions to the RAKAS

Channel networks and watershed boundaries were extracted for the RAK to examine runoff patterns and potential recharge scenarios in light of the distribution of outcrops of the various aquifers of the RAKAS. The Topographic Parameterization (TOPAZ) program of Garbrecht and Martz (1995) was used to extract the distribution of drainage networks and watersheds from Shuttle Radar Topography Mission

(SRTM) digital elevation data with 1 km spatial resolution (Fig. 3b). Elevation of each cell was compared to that of the neighboring cells, and the flow direction was assumed to be toward the cell with lowest elevation and all cells draining into one outlet were assumed to belong to the same watershed. Elevation data were smoothed to avoid generating false dams and pits by averaging elevations within individual cells. SRTM-derived streams and watersheds were calibrated and validated by comparison to co-registered Landsat and geologic maps. A major E–W trending watershed and its drainage networks was delineated; this watershed collects precipitation over the Red Sea Hills, and

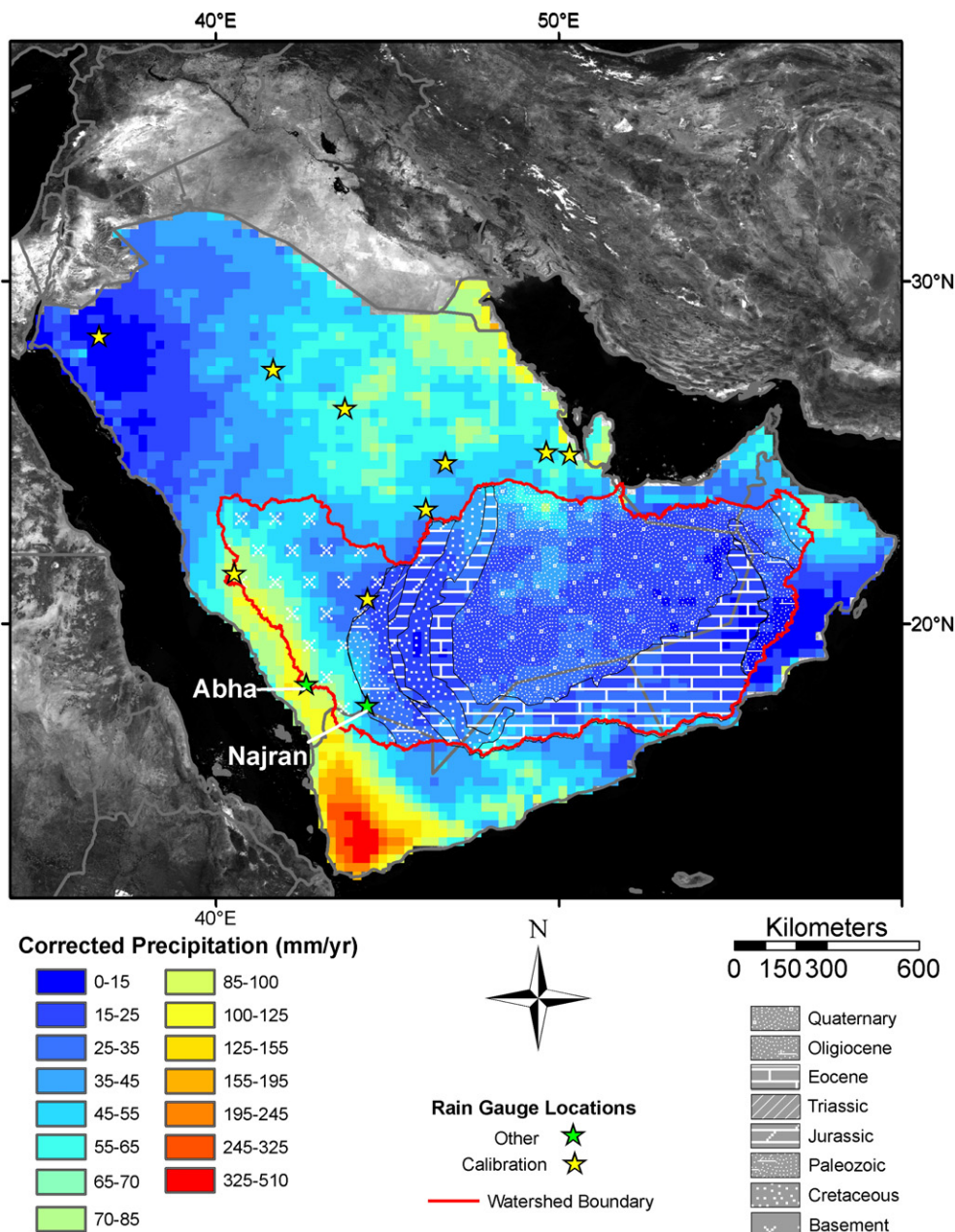


**Figure 9** Average (1998–2006) annual precipitation over the Arabian Peninsula extracted from 3-hourly TRMM precipitation data. Yellow star symbols represent the locations for the nine rain gauges that were used for calibrating the TRMM precipitation data. Also shown are locations of two additional stations (Abha and Najran), outline of the RAK watershed, and outcrops of the RAK aquifers and their postulated extensions under the sand cover.

cross cuts the RAK, potentially recharging its Paleozoic, Triassic, Cretaceous, and Tertiary aquifers cropping out at the foothills of the Red Sea Hills, and finally drains into the Arabian Gulf (Figs. 2, 3b, and 9). These conclusions are supported by the analysis of static head data from 156 wells that were drilled by Aramco.

There is a clear southwest to northeast decrease in static head for wells penetrating various aquifer systems in the RAK (Fig. 8a). Static water levels decrease from >900 m amsl at the foothills of the Red Sea mountain range to 300 m amsl at the central part of the RAK, approaching sea level in proximity of the Arabian Gulf (Fig. 8a). Because we do not observe similar south to north decreases in static head gradients, we conclude that the recharge of the RAKS is largely coming from precipitation over the Red Sea Hills.

The question of whether modern precipitation over the Red Sea Hills is contributing to recharge has been addressed by analyzing the satellite-based spatial and temporal precipitation data over the Arabian Peninsula. Precipitation over the RAK is scarce except for that occurring over the mountainous areas surrounding the study area. Relatively, high rainfall amounts occur orographically along the leeward sides of the mountains such as in the Asir (150 mm/yr), Abha (100 mm/yr), and Najran (80 mm/yr) regions of the Kingdom of Saudi Arabia (Fig. 9). Fig. 9 provides annual average precipitation data extracted from 3-hourly TRMM (Tropical Rainfall Measuring Mission) precipitation data over a period of nine years that was calibrated against field gauge data. The calibration was accomplished by multiplying each of the TRMM picture elements by an appropriate factor that will adjust the measured TRMM data to the observed value for the rain gauge within the same TRMM picture element. These factors were computed from the average annual precipitation (AAP) from each of the nine gauges and the respective values from TRMM data. For picture elements where no gauge data is available, the adjustment factors were computed using standard linear interpolation methods (i.e., inverse distance weighted method) applied to the known factor values for the nine stations.

The temporal and spatial analysis of global TRMM precipitation data sets over the RAK was enabled through the development and utilization of the recently developed Remote Sensing Data Extraction Model (RESDEM) (Milewski et al., 2007). Our analysis indicates that approximately  $150 \times 10^9 \text{ m}^3 \text{ a}^{-1}$  of rain precipitates over the Arabian Peninsula. Of this amount, approximately  $40 \times 10^9 \text{ m}^3 \text{ a}^{-1}$  falls over the RAK. A considerable portion (approximately,  $15 \times 10^9 \text{ m}^3 \text{ a}^{-1}$ ) of the precipitation over the RAK originates as rain over the Red Sea Hills that is channeled as inland drainage.

It has been demonstrated that recharge constitutes a considerable portion of precipitation in settings similar to those of the Empty Quarter. For example, Gheith and Sultan (2002) estimated that during a major storm in 1994, ground water recharge through transmission losses ranged from 21% to 31% of the precipitated volume over the Red Sea Hills for the major watersheds draining the Red Sea Hills in the northern parts of the Eastern Desert of Egypt. Using field experiment-based measurements acquired throughout the time period of 1983–1990, and applying a water balance approach, Abdulrazzak and Sorman (1994) and Abdulrazzak

(1995), estimated transmission losses in the Tabalah Basin, in the southwestern region of Saudi Arabia, at 15–25% of the precipitation volume. Using a chloride mass balance approach, Bazuhair and Wood (1996) measured recharge rates amounting to 12–20% of total precipitation in the alluvial aquifers in several wadis (Abha, Jazan) along the Red Sea Hills. Similar estimates (10–20% of total precipitation) were obtained for the Tharad and Yalamlam Wadis in Western Saudi Arabia (Subyani, 2004, 2005) using the same technique. Adopting recharge rates similar to those reported above (i.e., 10–25% of precipitated volume), we estimate average annual recharge rates for the RAK ranging from  $4 \times 10^9 \text{ m}^3 \text{ a}^{-1}$  to  $10 \times 10^9 \text{ m}^3 \text{ a}^{-1}$ .

## Summary and conclusions

A suite of groundwater samples was collected during an expedition organized by the Saudi Geological Survey in February/March 2006. Groundwater samples were collected from a variety of wells along the perimeter of the eastern half of the RAK (depths ranging from 1.5 to 800 m), including flowing artesian wells, pumped wells (formerly artesian), and shallow hand-dug wells encompassing sabkha areas.

Two groups of samples were identified on the basis of the hydrologic settings of the examined reservoirs and the chemical and isotopic characteristics of the samples: (1) Group 1 samples are from deep (>150 m deep) groundwater reservoirs and were collected from flowing artesian wells, pumped wells, and springs and (2) Group 2 samples are from shallow groundwater reservoirs (<15 m) and were collected from shallow production wells, hand-dug wells, and water points. Group 1 samples are isotopically depleted ( $\delta^2\text{H}$  values ranging from  $-60\text{‰}$  to  $-35\text{‰}$ ), but have total dissolved solids concentrations ranging from 1300 to 76,000 mg/L, indicating that much of the salinity is acquired in the subsurface from dissolution of marine evaporites and interaction with aquifer rock units along their flow paths. A likely source of salinity is the Hormoz Series, an Upper Proterozoic sedimentary sequence largely formed of bedded salt, gypsum, anhydrite, with thick interbeds of dolomite, shale, and sandstone. This scenario is supported by a general west to east increase in total salinity and the correlation between the distribution of samples with the highest salinities and the distribution of the Hormoz series at depth. These waters represent either high-elevation recharge from mountainous areas, and/or recharge largely formed of paleowater precipitated during moist climate intervals of the late Pleistocene.

Water from shallow hand-dug wells including those in sabkha areas (Group 2) has experienced significant evaporation ( $\delta^2\text{H}$  values ranging from  $-34\text{‰}$  to  $+19\text{‰}$ ) as well as salinization (TDS as high as 92,000 mg/L) by dissolution of sabkha salts including halite and gypsum. Stable isotope data for the Group 2 water samples define an evaporation trend line originating from the Group 1 water samples. This relationship indicates that the Group 2-type water evolved from 1-type water by ascending through structural discontinuities, dissolving evaporative salts, and undergoing substantial near-surface evaporation in groundwater discharge zones (sabkhas) characterized by shallow groundwater lev-

els (<2 m). This interpretation is supported by the relatively unradiogenic Sr isotope ratios of groundwater samples ( $Sr^{87}/Sr^{86} = 0.70771\text{--}0.70874$ ) that are consistent with Group 1 samples having interacted with Eocene aquifer rocks and Group 2 samples having interacted with overlying Neogene aquifer rocks. The Sr isotope ratios are significantly different from that of modern seawater ( $^{87}Sr/^{86}Sr = 0.70932$ ), indicating that seawater intrusion or inundation has not played a major role in sabkha formation.

Results point to a single recharge source for Group 1 and 2 samples, most likely the precipitation falling over the Red Sea Hills. This precipitation has significant potential for recharging the Paleozoic, Triassic, Cretaceous, and Eocene aquifers cropping out in the foothills of the Red Sea mountains to the east. This inference is supported by a progressive decrease in static heads from SW to the NE, substantial precipitation over the adjacent Red Sea Hills, and the presence of a major E–W trending drainage network that channels precipitation towards recharge areas to the east.

Although we believe that the RAKAS is largely formed of fossil water that was recharged during previous wet climatic periods, we suggest that during the intervening dry periods, as is the case now, these aquifers must receive some additional recharge. This has been demonstrated to be the case in similar settings in the Eastern Desert of Egypt and the Sinai Peninsula (Sultan et al., 2007). To obtain first order estimates for modern contributions to the RAKAS, we used the recently developed Remote Sensing Data Extraction Model to analyze global 3-hourly TRMM precipitation data sets acquired (1998–2006) over the Arabian Peninsula. Our analysis indicates that of the  $150 \times 10^9 \text{ m}^3 \text{ a}^{-1}$  of precipitation that constitutes the average annual precipitation over the Arabian Peninsula, approximately  $40 \times 10^9 \text{ m}^3 \text{ a}^{-1}$  are channeled towards the RAK. Adopting recharge rates (10–25% of precipitation volume) that were extracted for areas with similar climatic, hydrologic, geologic settings conditions in the Red Sea Hills and surroundings in Egypt and Saudi Arabia, we estimate an average annual recharge rate of  $4 \times 10^9 \text{ m}^3 \text{ a}^{-1}$  to  $10 \times 10^9 \text{ m}^3 \text{ a}^{-1}$  for the RAK. This compares with a current total estimated water usage of about  $22 \times 10^9 \text{ m}^3 \text{ a}^{-1}$  in Saudi Arabia.

Results show that groundwater resources in the RAK are apparently significant compared to other areas in the Arabian Peninsula and offer development potential that merits further detailed investigations. Development scenarios should preferentially target aquifers that are proximal to recharge areas to intercept groundwater before undergoing substantial dissolution of marine evaporites along their flow paths and before being subjected to near-surface evaporation in discharge areas. Additional integrated studies (e.g., modeling, geochemistry, geophysics, GIS) on recharge rates, sustainability, and water quality issues for the RAKAS could potentially demonstrate that the RAK is one of the most promising sites for groundwater exploration in the Arabian Peninsula. Results also highlight the importance of investigating the potential for sustainable exploitation of similar large aquifer systems that were largely recharged in previous wet climatic periods yet are still receiving modest modern meteoric contributions. Investigating and ultimately developing these aquifer systems could potentially provide partial solutions to the mounting water shortages in arid and hyper-arid regions.

## Acknowledgments

We thank the administration of the Saudi Geological Survey for arranging the field excursion to the RAK, all the geologists of the Saudi Geological Survey who organized and led this excursion, and the LBC for covering the excursion.

## References

- Abdulrazzak, M., 1995. Water supplies versus demand in countries of the Arabian Peninsula. *Journal of Water Resources Planning and Management*. v. May/June 1995.
- Abdulrazzak, M.J., Sorman, A.U., 1994. Transmission losses from ephemeral stream in arid region. *Journal of Irrigation and Drainage Engineering-Asce* 120, 669–675.
- Al Alawi, J., Abdulrazzak, M., 1994. Water in the Arabian Peninsula: problems and perspectives. In: Rogers, P., Lydon, P. (Eds.), *Water in the Arab World; Perspectives and Prognoses*. Harvard University Press, pp. 171–202.
- Allison, G.B., 1982. The relationship between oxygen-18 and deuterium in water in sand columns undergoing evaporation. *Journal of Hydrology* 55, 163–169.
- AlSharhan, A.S., 2003. Petroleum geology and potential hydrocarbon plays in the Gulf of Suez rift basin, Egypt. *AAPG Bulletin* 87, 143–180.
- AlSharhan, A.S., Nairn, A.E.M., 1997. *Sedimentary Basins and Petroleum Geology of the Middle East*. Elsevier Science, 942 p.
- AlSharhan, A.S., Rizk, Z.A., Nairn, A.E.M., Bakhit, D.W., AlHajari, S.A., 2001. *Hydrogeology of an Arid Region. The Arabian Gulf and Adjoining Areas*. Elsevier, Amsterdam.
- Appelo, C.A.J., 1994. Some calculations on multicomponent transport with cation-exchange in aquifers. *Ground Water* 32, 968–975.
- Bazuhair, A., Wood, W., 1996. Chloride mass-balance method for estimating ground water recharge in arid areas: examples from Western Saudi Arabia. *Journal of Hydrology* 186, 153–159.
- Beaumont, P., 1977. Water development in Saudi Arabia. *The Geographical Journal* 143, 42–60.
- Burns, S.J., Fleitmann, D., Matter, A., Kramers, J., Al-Subbary, A.A., 2003. Indian Ocean climate and an absolute chronology over Dansgaard/Oeschger events 9 to 13. *Science* 301, 1365–1367.
- Chapelle, F.H., Knobel, L.L., 1983. Aqueous geochemistry and the exchangeable cation composition of glauconite in the Aquia Aquifer, Maryland. *Ground Water* 21, 343–352.
- Clark, I.D., Fritz, P., 1997. *Environmental Isotopes in Hydrogeology*. CRC Press/Lewis Publishers, Boca Raton, FL, 328 p.
- Coleman, M.L., Shepherd, T.J., Durham, J.J., Rouse, J.E., Moore, G.R., 1982. Reduction of water with zinc for hydrogen isotope analysis 54, 993–995.
- Coplen, T.B., 1996. New guidelines for the reporting of stable hydrogen, carbon, and oxygen isotope ratio data. *Geochimica et Cosmochimica Acta* 60, 3369.
- Craig, H., 1961. Isotopic variations in meteoric waters. *Science* 133, 1702–1703.
- Dansgaard, W., 1964. Stable isotopes in precipitation. *Tellus* 16, 436–468.
- Depaolo, D.J., Finger, K.L., 1991. High-resolution strontium-isotope stratigraphy and biostratigraphy of the miocene-monterey-formation, Central California. *Geological Society of America Bulletin* 103, 112–124.
- Depaolo, D.J., Ingram, B.L., 1985. High-resolution stratigraphy with strontium isotopes. *Science* 227, 938–941.
- Dewdney, J., 1988. *The Cambridge Atlas of the Middle East and North Africa*. Cambridge University Press, UK, 74pp.

- Dimock, W.C., 1961, A Study of the Water Resources of the Rub Al-Khali in Southern Saudi Arabia. Unpublished Groundwater Report 22, ARAMCO, p. 183.
- Edgell, H.S., 1991. Proterozoic salt basins of the Persian Gulf area and their role in hydrocarbon generation. *Precambrian Research* 54, 1–14.
- Fleitmann, D., Burns, S.J., Mudelsee, M., Neff, U., Kramers, J., Mangini, A., Matter, A., 2003a. Holocene forcing of the Indian monsoon recorded in a stalagmite from Southern Oman. *Science* 300, 1737–1739.
- Fleitmann, D., Burns, S.J., Neff, U., Mangini, A., Matter, A., 2003b. Changing moisture sources over the last 330,000 years in Northern Oman from fluid-inclusion evidence in speleothems. *Quaternary Research* 60, 223–232.
- Fleitmann, D., Burns, S.J., Neff, U., Mudelsee, M., Mangini, A., Matter, A., 2004. Palaeoclimatic interpretation of high-resolution oxygen isotope profiles derived from annually laminated speleothems from Southern Oman. *Quaternary Science Reviews* 23, 935–945.
- Garbrecht, J., Martz, L., 1995. TOPAZ: An Automated Digital Landscape Analysis Tool for Topographic Evaluation, Drainage Identification, Watershed Segmentation, and Sub-Catchment Parameterization: Overview: Agricultural Research Service v. NAWQL 95.
- Gheith, H., Sultan, M., 2002. Construction of a hydrologic model for estimating wadi runoff and groundwater recharge in the eastern desert, Egypt. *Journal of Hydrology* 263, 36–55.
- Glennie, K.W., 1970. *Desert Sedimentary Environments*. Elsevier, Amsterdam, 222 p.
- Hess, J., Bender, M., Schilling, J.G., 1991. Assessing seawater basalt exchange of strontium isotopes in hydrothermal processes on the flanks of Mid-ocean ridges. *Earth and Planetary Science Letters* 103, 133–142.
- IAEA, I.A.E.A., and WMO, W.M.O., 2004, Global Network for Isotopes in Precipitation, The GNIP database.
- Issar, A.S., Bruins, H.J., 1983. Special climatological conditions in the deserts of Sinai and the Negev during the latest pleistocene. *Palaeogeography, Palaeoclimatology, Palaeoecology* 43, 63–72.
- Leuschner, D.C., Sirocko, F., 2000. The low-latitude monsoon climate during Dansgaard–Oeschger cycles and Heinrich Events. *Quaternary Science Reviews* 19, 243–254.
- Macumber, P.G., Al-Said, S.B.G., Kew, G.A., Tennakoon, T.B., 1994. Hydrogeologic implications of a cyclonic rainfall event in central Oman. In: Nash, H., McCall, G.J.H. (Eds.), *Groundwater Quality*. Chapman & Hall, pp. 87–97.
- Matter, J.M., Waber, H.N., Loew, S., Matter, A., 2006. Recharge areas and geochemical evolution of groundwater in an alluvial aquifer system in the Sultanate of Oman. *Hydrogeology Journal* 14, 203–224.
- McClure, H.A., 1978. Early paleozoic glaciation in Arabia. *Palaeogeography, Palaeoclimatology, Palaeoecology* 25, 315–326.
- McClure, H.A., 1980. Permian–carboniferous glaciation in the Arabian Peninsula. *Geological Society of America Bulletin* 91, 707–712.
- Milewski, A., Sultan, M., Balekai, R., Markondiah Jayaprakash, S., Becker, R., 2007. RESDEM, A vehicle for data mining and modeling of temporal remote sensing data (TRMM, SSM/I, AVHRR, AMSR, MODIS, and QuikSCAT). In: *Geological Society of America Annual Meeting Abstracts with Programs* 39.
- Ministry of Higher Education, S.A., 2000. Atlas of Saudi Arabia. Saudi Arabian Ministry for Higher Education.
- Otkun, G., 1971, Paleozoic sandstone aquifers in Saudi Arabia. In: *International Association of Hydrogeologists: Tokyo Congress*.
- Poage, M.A., Chamberlain, C.P., 2001. Empirical relationships between elevation and the stable isotope composition of precipitation and surface waters, Considerations for studies of paleoelevation change. *American Journal of Science* 301, 1–15.
- Powers, R.W., Ramirez, L.F., Redmond, C.D., Elberg, E.L.J., 1966. *Geology of the Arabian Peninsula*. U.S. Geologic Survey, Professional Paper 560-D, p. 127.
- Preusser, F., Radies, D., Matter, A., 2002. A 160,000-year record of dune development and atmospheric circulation in southern Arabia. *Science* 296, 2018–2020.
- Socki, R.A., Karlsson, H.R., Gibson, E.K., 1992. Extraction technique for the determination of O-18 in water using preevacuated glass vials. *Analytical Chemistry* 64, 829–831.
- Sturchio, N.C., Arehart, G.B., Sultan, M., Sano, Y., AboKamar, Y., Sayed, M., 1996. Composition and origin of thermal waters in the Gulf of Suez area, Egypt. *Applied Geochemistry* 11, 471–479.
- Subyani, A., 2004. Use of chloride mass-balance and environmental isotopes for evaluation of groundwater recharge in the Alluvial Aquifer, Wadi Tharad, Western Saudi Arabia. *Environmental Geology* 46, 741–749.
- Subyani, A., 2005. Hydrochemical identification and salinity problem of ground-water in Wadi Yalamlam Basin, Western Saudi Arabia. *Journal of Arid Environments* 60, 53–66.
- Sultan, M., Yan, E., Sturchio, N., Wagdy, A., Gelil, K.A., Becker, R., Manocha, N., Milewski, A., 2007. Natural discharge: a key to sustainable utilization of fossil groundwater. *Journal of Hydrology* 335, 25–36.
- USGS, Aramco, 1963. *Geological Map of the Arabian Peninsula, Miscellaneous Geologic Investigations Map I-270A*. Ministry of Petroleum and Mineral Resources.
- Weyhenmeyer, C.E., Burns, S.J., Waber, H.N., Macumber, P.G., 2002. Isotope study of moisture sources, recharge areas, and groundwater flow paths within the eastern Batinah coastal plain, Sultanate of Oman. *Water Resources Research*, 38.